RESEARCH ARTICLE | MAY 22 2014

Binding of solvated peptide (EPLQLKM) with a graphene sheet via simulated coarse-grained approach

Somayyeh Sheikholeslami; R. B. Pandey; Nadiya Dragneva; Wely Floriano; Oleg Rubel; Stephen A. Barr; Zhifeng Kuang; Rajiv Berry; Rajesh Naik; Barry Farmer

J. Chem. Phys. 140, 204901 (2014)
https://doi.org/10.1063/1.4876716

Binding of solvated peptide (EPLQLKM) with a graphene sheet via simulated coarse-grained approach

Somayyeh Sheikholeslami,[1] R. B. Pandey,[1] Nadiya Dragneva,[2] Wely Floriano,[2] Oleg Rubel,[2] Stephen A. Barr,[3] Zhifeng Kuang,[3] Rajiv Berry,[3] Rajesh Naik,[3] and Barry Farmer[3]

[1]*Department of Physics and Astronomy, University of Southern Mississippi, Hattiesburg, Mississippi 39406-0001, USA*

[2]*Thunder Bay Regional Research Institute and Lakehead University, 955 Oliver Road, Thunder Bay, Ontario P7B 5E1, Canada*

[3]*Materials and Manufacturing Directorate, Air Force Research Laboratory, Wright Patterson Air Force Base, Ohio 45433, USA*

(Received 11 January 2014; accepted 4 May 2014; published online 22 May 2014)

Binding of a solvated peptide A1 (^{1}E ^{2}P ^{3}L ^{4}Q ^{5}L ^{6}K ^{7}M) with a graphene sheet is studied by a coarse-grained computer simulation involving input from three independent simulated interaction potentials in hierarchy. A number of local and global physical quantities such as energy, mobility, and binding profiles and radius of gyration of peptides are examined as a function of temperature (T). Quantitative differences (e.g., the extent of binding within a temperature range) and qualitative similarities are observed in results from three simulated potentials. Differences in variations of both local and global physical quantities suggest a need for such analysis with multiple inputs in assessing the reliability of both quantitative and qualitative observations. While all three potentials indicate binding at low T and unbinding at high T, the extent of binding of peptide with the temperature differs. Unlike un-solvated peptides (with little variation in binding among residues), solvation accentuates the differences in residue binding. As a result the binding of solvated peptide at low temperatures is found to be anchored by three residues, ^{1}E, ^{4}Q, and ^{6}K (different from that with the un-solvated peptide). Binding to unbinding transition can be described by the variation of the transverse (with respect to graphene sheet) component of the radius of gyration of the peptide (a potential order parameter) as a function of temperature. © *2014 AIP Publishing LLC*. [http://dx.doi.org/10.1063/1.4876716]

I. INTRODUCTION

Understanding the peptide binding to a graphene sheet[1–3] has attracted a considerable interest in recent years primarily due to its vast potential in designing bio-functionalized nanomaterials.[4–10] Kim *et al.*[2] have recently reported an unusual edge-binding characteristic of a peptide A1 (EPLQLKM) to graphene which not only binds more than that of its mutations but also leads to different surface morphology as a result. Computer simulations involving all-atom Molecular Dynamics (MD) as well as coarse-grain approaches are performed to probe binding further.[11,12] Because of the limitations of the tools including force-fields, verification of experimental observations is still illusive. All-atom MD simulations with atomistic details provide useful insight into its binding of peptide with the identification of underlying atoms in anchoring and residues in simplified systems (e.g., dilute solution with few peptides at an ambient temperature). Coarse-grained simulations, on the other hand, can be carried out for a range of temperature with a variety of peptides with relatively more ease to understand the large-scale binding characteristics. There are many ways to coarse-graining.[11,13–20] However, the properties under investigation and its reliability depend on the choice of coarse-grain interactions (e.g., residue-residue, residue-solvent, residue-substrate, etc.) and incorporate pertinent characteristics of the constitutive elements (e.g., residues and peptides).

Binding of peptide A1 and its mutations with a graphene sheet has been very recently examined by a hierarchical coarse-grained approach without the presence of solvent.[11,12] Residue-graphene and residue-residue interactions are involved in this study.[11] The residue-graphene interaction, critical in binding, can be estimated by an all-atom MD simulations.[11] The residue-residue interactions can be similarly estimated from simulations involving atomistic scale details.[16] Additionally, alternate methods such as hydropathy-index[11,12] and knowledge-based residue-residue contact matrices[21–27] can also be used to estimate interactions among the residues. In some of our recent studies of peptide-graphene binding, residue-residue interactions are based on hydropathy index.[11,12] We would like to constrain to the same approach (hydropathy index) for the residue-residue interactions to investigate the binding of peptide A1 with the graphene. However, unlike the previous studies, we would like to consider solvated systems as the solvent plays a critical role in modulating the interactions of the underlying residues.[28–30] Very recently, residue-graphene interactions have been evaluated with three independent all-atom MD simulations in presence of solvent.[11,31,32] These simulated data for the solvated residue-graphene interactions can be used as input to a coarse-grain approach in hierarchy similar to previous studies in absence of solvent.[11,12] The model is presented in Sec. II followed by results and discussion in Sec. III and concluding remarks in Sec. IV.

II. MODEL AND METHOD

The simulation box consists of a number of peptide chains with a graphene sheet positioned at the center. A peptide chain is a set of residues (amino acids) tethered together via flexible covalent bonds in a specific sequence (E-P-L-Q-L-K-M). Each amino acid is unique with its characteristic side chain anchored by C-alpha at the center with amine and carboxylic acid group at the opposite ends. Even with a relatively small number of atoms (order of 10–27), the degrees of freedom (torsional, covalent elastic bonds, translational) associated with an amino acid are appreciably large. The degrees of freedom associated with a peptide chain are accordingly enhanced with the number of underlying amino acids at the atomic scale; the number of chains (in many applications) further increases the multiplicity in degrees of freedom. Covering the huge conformational phase space in a large-scale simulation (usually needed to estimate equilibrium thermodynamic properties) requires large time steps; analysis of many local and global physical quantities by all-atom MD simulations alone may not be feasible.

Unique characteristics of each amino acid (embedded in its atomic scale structure) are also critical in exploring the versatility and specificity of peptides, its assembly, and binding. Therefore, some degree of coarse-graining, i.e., reducing the degrees of freedom and/or adopting efficient and effective procedures while preserving the pertinent characteristics, becomes a necessity in order to perform large-scale computer simulations. Recent years have witnessed an explosive growth towards developing coarse-grained models involving both Monte Carlo (MC) and Molecular Dynamics methods. We have been using a multi-scale approach that utilizes the input of results from all-atom simulations in a coarse-grained representation of peptide with an efficient computational model in a hierarchical fashion to investigate large-scale properties.

A. Binding of amino acids with the graphene

All-atom MD simulations with amino acids (AAs) and a graphene sheet in the box can be performed to assess their binding energy which is a measure of its unique interaction with the graphene. Binding energy of amino acids has been recently examined by several research groups with different surfaces. For example, Nawrocki and Cieplak[33] have studied the binding of amino acids and protein at the ZnO-water interface and Feng *et al.*[34] have estimated the binding of amino acids on gold surfaces. Binding of amino acids with the graphene in aqueous solution has been extensively examined by three all-atom MD simulations.[11,31,32] Figure 1 shows the normalized binding energy from these three independent studies. Despite similarity in general binding features (i.e., most binding residues W(tryptophan, trp), Y(tyrosine, tyr), R(arginine, arg)), there are some differences. For example, cysteine (C, cys) appears to bind readily with graphene in data from Pandey *et al.*[11] in contrast to results from Camden *et al.*[31] while reverse seem to be the case for F(phenylalanine, phe). Fluctuation in binding energy (i.e., variation in the average estimate among 20 amino acids) is generally higher in the data by Pandey *et al.*[11] and Camden *et al.*[31] than that from Dragneva *et al.*[32] Such discrepancies in results are common in all-atom MD simulations, as the results are sensitive to type of the force field and its implementation. Lower binding energy of residues with the graphene surface in presence of solvent is due to presence of explicit solvent molecules between the amino acids and the substrate as pointed out by Dragneva *et al.*[32] Thus, it is a good to look at results from independent simulations particularly when it

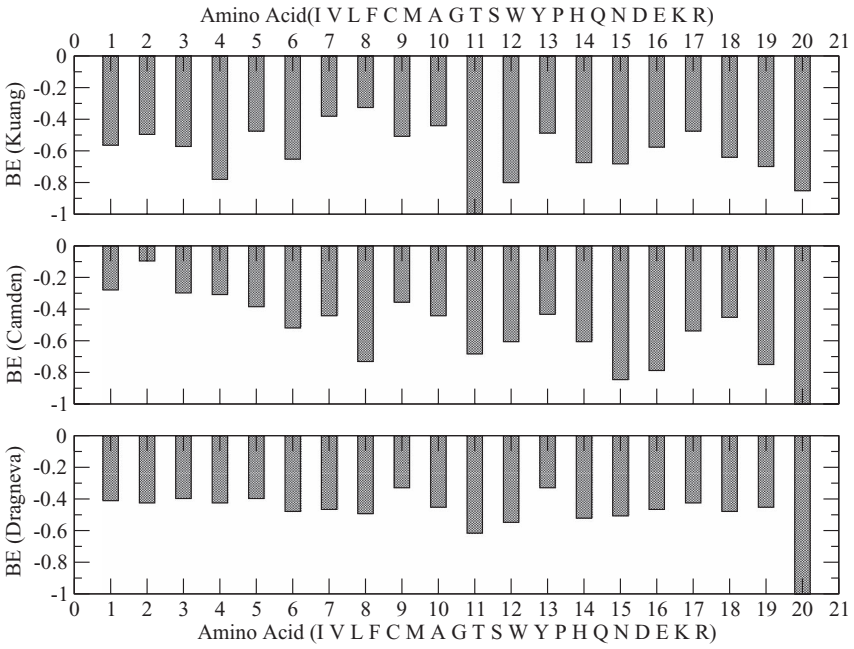

FIG. 1. Normalized binding energy of 20 amino acids (AAs) with the graphene sheet in presence of solvent from three independent all-atom MD simulations (Kuang,[11] Camden,[31] and Dragneva[32]).

is used as input (follows) to such hierarchical coarse-grained modeling as the one used here.

B. Coarse-grained approximation

In our coarse-grained description,[11] a residue is represented by a node (particle), i.e., the structural detail of the residue (at atomic scale) is ignored. The peptide is described by a set of seven nodes tethered together via peptide (covalent) bonds, ^{1}E-^{2}P-^{3}L-^{4}Q-^{5}L-^{6}K-^{7}M. On a cubic lattice grid, a node occupies a cube (eight lattice sites) and the bond length between consecutive nodes can vary (fluctuate) between 2 and $\sqrt{10}$ in unit of lattice constant. Such bond fluctuation methods[35] are extensively used in studying the structure and dynamics of homo-polymer systems,[36] multi-component nano-composites,[8,9] and protein chains[29,30] and is known[36] for its computational efficiency with ample degrees of freedom. A generalized Lennard-Jones potential is used for the residue-residue and residue-graphene interactions,

$$U_{ij} = \left[|\varepsilon_{ij}| \left(\frac{\sigma}{r_{ij}}\right)^{12} + \varepsilon_{ij} \left(\frac{\sigma}{r_{ij}}\right)^{6} \right], r_{ij} < r_c, \qquad (1)$$

where r_{ij} is the distance between the residue at site i and another residue or graphene at site j; $r_c = \sqrt{8}$ is the range of interaction and $\sigma = 1$ in units of lattice constant. Strength ε_{ij} (a measure of the depth) of the potential is unique for the interaction of each residue (node) with the substrate and other residues. The interaction between residue of the peptide and the substrate is critical in binding of peptides with the graphene. Data from three independent MD simulations (Figure 1) are used as input for ε_{ij}. Estimates for the residue-residue interaction (ε_{ij}) are based on the hydropathy index. It involves a generalized interaction between hydrophobic (h), polar (p), and electrostatic (e) residues, i.e., $\varepsilon_{hh} = -0.1$, $\varepsilon_{pp} = -0.2$, $\varepsilon_{pe} = -0.2$; the interactions (ε_{ee}) between the electrostatic residues (E, K) $\varepsilon_{EE} = \varepsilon_{KK} = 0.1$, $\varepsilon_{EK} = -0.4$. Among each group (h, p, e) the residue-residue interactions are weighted by their hydropathy index[9,11] which makes each residue-residue pair interaction unique. Residue-graphene interactions are generally much stronger (see Figure 1) than the residue-residue interactions and therefore play a critical role in understanding the peptide binding with the graphene substrate. As pointed out above, there are few more choices for residue-residue interaction (consisting of an interaction matrix with 210 elements for 20 AAs) such as simulation-based residue-residue interaction,[16] knowledge-based residue-residue interaction[21–30] which are used extensively in study of protein folding. We have selected the phenomenological residue-residue interaction potential based on hydropathy index of the AAs because we wanted to use the same interactions used in our un-solvated simulations[11] for consistency and comparison.

C. Simulation procedure

The computer simulation[11] is set up on a cubic lattice (L^3) with the graphene sheet fixed at the center. Peptide chains with a concentration C_p (which is the volume fraction occupied by its residues) are then inserted randomly in the simulation box to perform their stochastic motion. Each residue in each peptide chain executes its stochastic movement with the Metropolis algorithm subject to constraints imposed by the excluded volume and the limitations on changes in the covalent bond length. That is, a randomly selected residue of a randomly selected peptide chain is moved from a site i to site j with the Boltzmann probability $\exp(-\Delta E_{ij}/T)$, where ΔE_{ij} is the change in energy between its new (E_j) and old (E_i) configuration $\Delta E_{ij} = E_j - E_i$ and T is the temperature in reduced units (ε_{ij}/k_B) of the energy (ε_{ij}) and the Boltzmann constant (k_B). Because of the specificity of the interaction energy (ε_{ij}), the magnitude of the reduced temperature is different for different residue while the absolute temperature $T_a = T\ k_B/\varepsilon_{ij}$ remains the same. Unfortunately, we are unable to provide the absolute unit due to lack of experimental measurement of the appropriate physical quantities for calibration. The unit Monte Carlo step (MCS) is defined by attempts to move each residue once. Parameters and variables such as temperature, interaction energy, time, etc., are in arbitrary units to identifying the trends, i.e., the changes in variation of the observables; the units of the all-atom simulations can however be used to assess their order of magnitude since it is used as input for the constitutive component.

The estimates of adsorption energy of residues in all-atom simulations are typically at the room temperature (300 K) in equilibrium.[11] The relative values of the adsorption energy of each residue is used as input in our phenomenological interaction potential via parameter ε_{ij} to assess relative binding of peptides and its residues qualitatively. Note that, in all-atom MD simulations, there may be some dependence of the absolute values of the adsorption energy on the temperature, estimates of its relative value however should not affect our result. Since a residue is represented by a unit cube of the underlying lattice space (see above), the magnitude of the reduced lattice constant is therefore comparable to the size of a residue (~3−10 A ~0.5 nm). The simulation box of size 100^3 in dimensionless unit is comparable to similar size in unit of nm^3. A typical estimate of the time to relax a residue in all-atom MD simulation is in the range from picosecond to nanosecond; 40 ns is used to relax residues in Ref. 11. If we use 40 ns as MCS unit; a 10^6 time step in MC simulation is equivalent to about 0.01 s. Order of magnitude of the temporal and spatial scales in observable units is just an estimate and should not be used for quantitative comparison with the laboratory data. Variations in relative binding of peptides as a function of temperature should be comparable to results from appropriate experimental observations. Within the limitation of the model our results could be used to interpret the laboratory observations.

III. RESULTS AND DISCUSSION

We analyze both local and global physical quantities to assess the binding of peptide with the graphene sheet as a function of temperature with the input of three independent simulated interaction potentials described above. It is worth reminding that the generalized potential for the residue-graphene and residue-residue interactions are

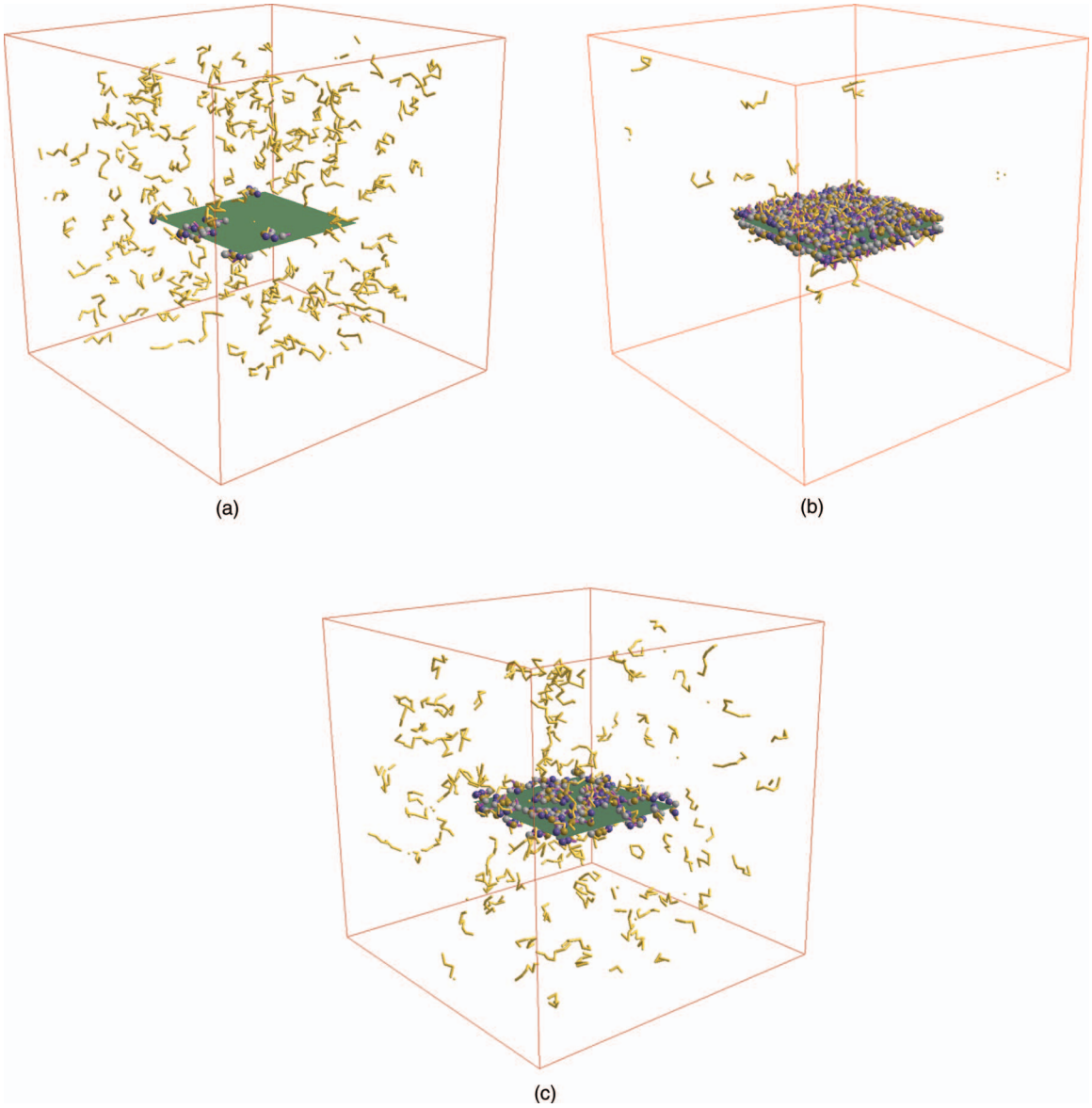

FIG. 2. Representative snapshots at the temperature T = 0.012 ((a), (b)) and 0.020 (c) (in unit of ε_{ij}/k_B) with the peptide concentration $C_p = 0.010$ at the time steps $t = 10^3$ (a) and 10^6 steps (b, T = 0.012 and c, T = 0.020). Graphene sheet (24^2) is at the center of the box (100^3). Residues that are bound to graphene are shown by spheres (grey (hydrophobic), golden (polar), blue (electrostatic)) with corresponding bonds (magenta). Free peptide chains are golden. The binding energy of AAs with the graphene from Ref. 32 is used as input for the simulated interaction potential (Figure 1) in coarse-grained interaction potential (Eq. (1)) to generate these snapshots.

phenomenological. Figure 2 shows typical snapshots at a low (T = 0.012) and a high (T = 0.020) temperature. At short times, i.e., $t = 10^3$ steps, the peptide chains are highly disperse (closer to initial random distribution) with few chains bound by some of their residues at T = 0.012. As simulation proceeds more chains come in contact with the graphene sheet and become adsorbed. In the asymptotic (long) time regime ($\sim 10^6$ step) most of the chains are adsorbed at such a low temperature (Figure 2(b), T = 0.012). Adsorption reduces on increasing the temperature to T = 0.020 (see Figure 2(c)). As expected, adsorption is enhanced on reducing the temperature while desorption becomes more prevalent on raising the temperature. Visual analysis of snapshots and animation provide a general idea about the adsorption and desorption as a function of time step and temperature. In order to quantify the extent of adsorption, identify the residue that anchors the binding, and the rate of adsorption, it is desirable to examine some of the local and global physical quantities (follows).

Figure 3 shows the energy profile of residue which is the average equilibrium energy of each residue (bound or unbound) at two temperatures T = 0.010 and 0.016 in unit of ε_{ij}/k_B. We see that the proline (^{2}P) has the lowest energy with all three potentials. Minimum energy does not necessarily mean strongest binding (see below). Estimate of energy involves average over all residues in each peptide with residue-residue and residue-graphene interaction energy within the range of interaction in asymptotic (equilibrium) time regime.

Mobility of each residue is also analyzed along with the global mobility of each peptide. Mobility (M_n) of a residue is defined as the average number of its successful moves.

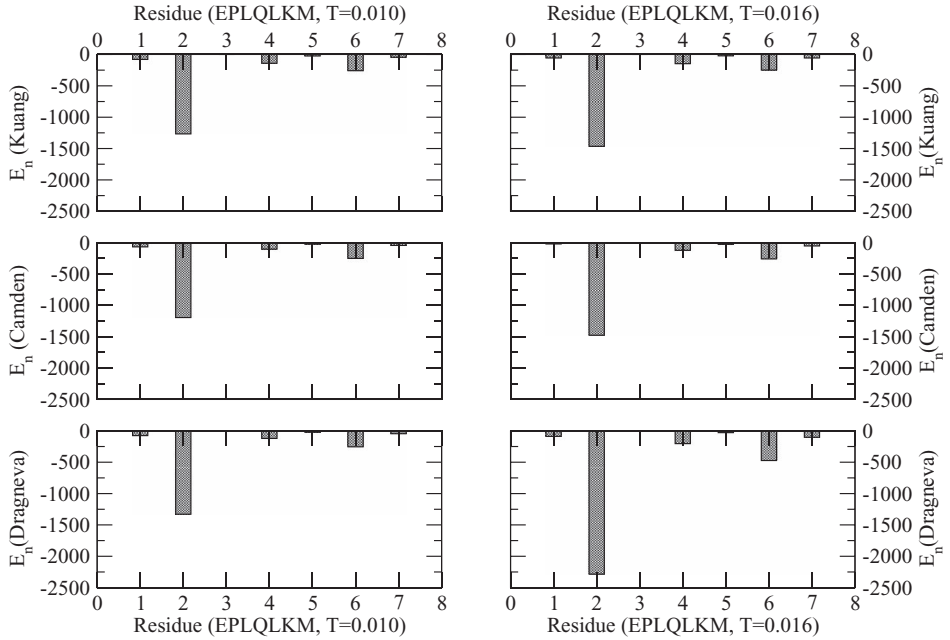

FIG. 3. Energy profile of peptide at two temperatures (T = 0.010, 0.016 in unit of ε_{ij}/k_B) with the input from three simulated interaction potentials, Kuang,[11] Camden,[31] and Dragneva[32] (Figure 1). E_n is the average energy (in arbitrary unit) of each residue. Lattice of size 100^3 with a 24^2 sheet at the center is used with the concentration of peptides $C_p = 0.01$ and 100 independent realizations each for a 10^6 time steps.

Figure 4 shows the mobility profile of the peptide at two representative temperatures (corresponding to Figure 3). Most of the peptides are adsorbed at low temperatures (e.g., T = 0.010) as seen in our visual animations (see also Figure 2). Lowest mobility for ^{4}Q and ^{6}K with all three potential suggests that these residues are most likely anchoring the peptide binding. Even though the mobility of each residue increases on raising the temperature to T = 0.016, the residues ^{4}Q and ^{6}K remain least mobile with all three potentials. The magnitude of the change in mobility however varies from one potential to another but the distinction in residue mobility is clear enough to identify the anchoring residues. Raising the temperature to high value (e.g., T = 0.028) leads to high mobility for each residue when the binding ceases to occur and distinction in residue mobility vanishes. It should be pointed out that the higher mobility of ^{7}M is not only due to competition between its interaction and temperature alone but also due to its position at the end in the sequence with relatively least

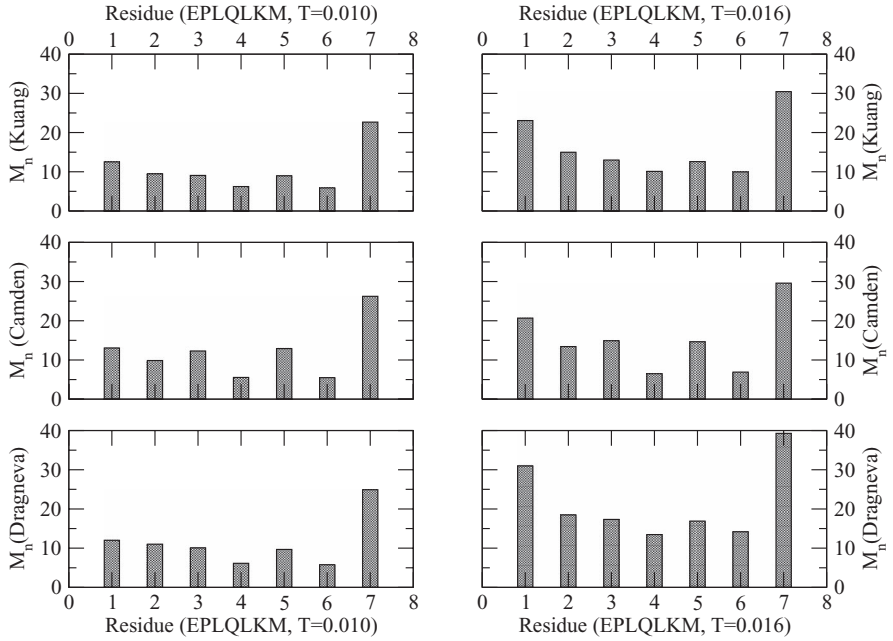

FIG. 4. Mobility (average number of successful move) profile of peptide at two temperatures (T = 0.010, 0.016 in unit of ε_{ij}/k_B) with the input from three simulated interaction potentials, Kuang,[11] Camden,[31] and Dragneva.[32] Lattice of size 100^3 with a 24^2 sheet at the center is used with the concentration of peptides $C_p = 0.01$ and 100 independent samples, each for a 10^6 time steps.

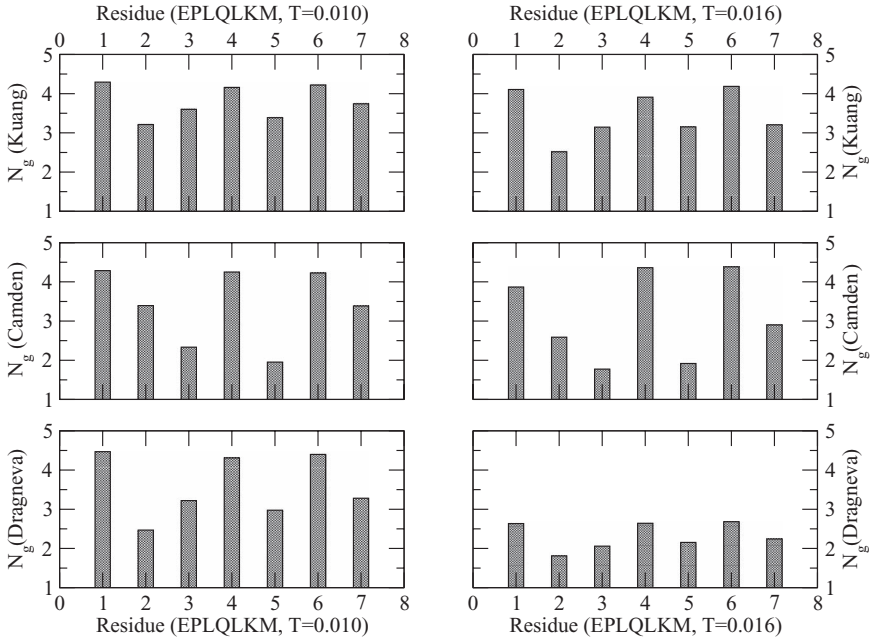

FIG. 5. Surface binding (average number of graphene sites within the range of interaction) profile of peptide at two temperatures (T = 0.010, 0.016 in unit of ε_{ij}/k_B) with the input from three simulated interaction potentials, Kuang,[11] Camden,[31] and Dragneva.[32] Lattice of size 100^3 with a 24^2 sheet at the center is used with the concentration of peptides $C_p = 0.01$ and 100 independent samples each for a 10^6 time steps.

constraint by only one covalent bond. Lowest connectivity is also providing higher mobility to residue ^{1}E at the other end of the peptide chain.

As the peptide is adsorbed its contact with the graphene sheet is enhanced. The average number (N_g) of graphene sites around each residue within the range of interaction in equilibrium can provide the strength of its binding. As in all estimates, the average is performed over the time steps (last one-third) in equilibrium and the number of independent samples at each temperature. The larger value of N_g for a residue obviously implies its higher probability of binding with the graphene and is a measure of the characteristic binding profile of the peptide. Binding profiles of the peptide with three simulated interaction potentials are presented in Figure 5. There are similarities and differences in the binding profiles with different simulated potentials. Binding of peptide A1 to

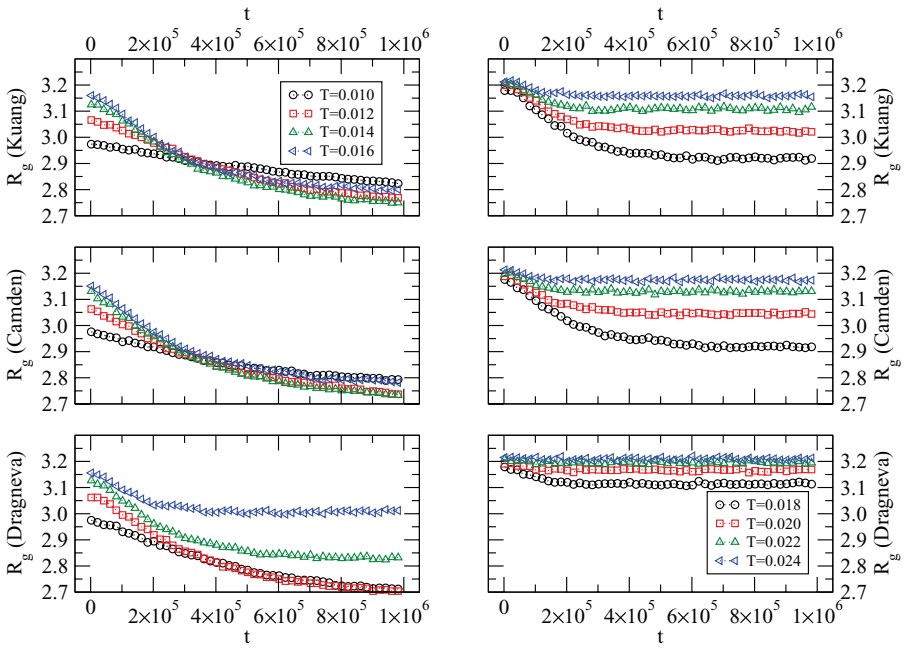

FIG. 6. Variation of the average radius of gyration (R_g) of the peptide in time at various temperatures in the range of T = 0.010–0.024 (in unit of ε_{ij}/k_B) with the input from three simulated interaction potentials, Kuang,[11] Camden,[31] and Dragneva.[32] Lattice of size 100^3 with a 24^2 sheet at the center is used with the concentration of peptides $C_p = 0.01$ and 100 independent samples each for a 10^6 time steps.

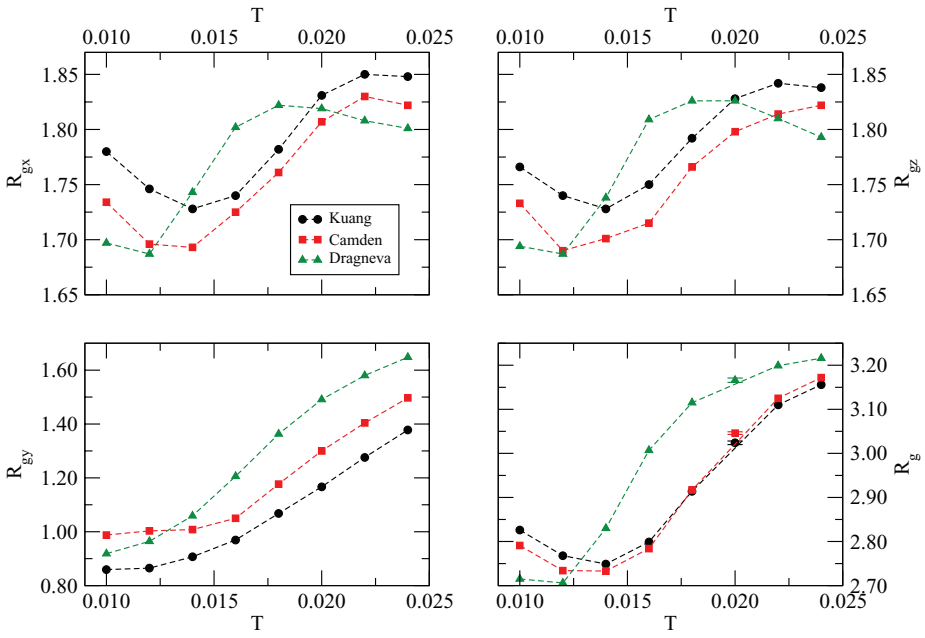

FIG. 7. Variation of the average equilibrium radius of gyration (R_g) and its components (R_{gx}, R_{gy}, R_{gz}) of the peptide A1 with the temperatures (in unit of ε_{ij}/k_B) with three simulated interaction potentials, Kuang,[11] Camden,[31] and Dragneva.[32] Lattice of size 100^3 with a 24^2 sheet at the center is used with the concentration of peptides $C_p = 0.01$ and 100 independent samples each for a 10^6 time steps. The statistical error bar is of the order of symbols; a representative value for R_g at $T = 0.020$ is shown.

graphene sheet is anchored by three residues, ^{1}E, ^{4}Q, and ^{6}K—a common feature of three potentials considered here. Note that ^{1}E remains bound to graphene despite its higher mobility than that of ^{4}Q and ^{6}K (see Figure 4). The binding profile of the solvated peptide A1 is very different from that of the un-solvated peptide (see Refs. 11 and 12) where little distinction exists in binding profile of residues. Although the solvation reduces the interaction[32] between the residues and the graphene it accentuates the distinction in their binding. The binding is reduced on increasing the temperature; the thermal response is highest with Dragneva potential.[31] Let us look closely into the differences. With the Kuang potential,[11] probability of binding of the remaining residues (^{3}L, ^{5}L, ^{7}M) is relatively high while the probability of anchoring by ^{3}L and ^{5}L with Camden potential[31] and that by ^{2}P with Dragneva potential[32] is relatively low.

Differences in binding profiles with the three simulated potential may affect the conformation and therefore the average radius of gyration of the peptides that are bound to graphene sheet. Binding of peptides depends on temperature (with the binding is more prevalent at lower temperatures) which should be reflected in response of the radius of gyration. Variation of the radius of gyration with the time steps is presented in Figure 6 for a range of temperatures (low-to-high) with three simulated interactions. We see that the radius of gyration reaches steady-state particularly at moderate to high temperature; approach to near-equilibrium at low temperatures is good enough to assess its relative thermal response and differences in results from three simulated interactions. Response of the radius of gyration is relatively similar with Kuang[11] and Camden[31] potentials and differs somewhat from the data with the Dragneva[32] potential. Apart from the shift in the temperature range, the nature of the temporal variation of R_g with temperature remains somewhat similar with all three. The graphene sheet is fixed at the center of the simulation box in zx-plane. Therefore, the transverse (y) component of the radius of gyration should be more affected due to binding than (x or z). We have analyzed the temporal variation of the transverse component of the radius of gyration and found that the pattern shares similar thermal response as the total radius of gyration.

Variation of the equilibrium radius of gyration and its components (x, y, z) with the temperature is presented in Figure 7 with three simulated interaction potentials. Thermal response of x and z components of the radius of gyration is different from that of its transverse (y) component. Apart from the shift in temperature range, the general response is relatively similar (z, x). As the binding reduces with the temperature, transverse component of the gyration radius increases accordingly rather linearly with the temperature. It is tempting to identify the radius of gyration (R_g) as an order parameter of binding transition due to its continuous decay with the temperature, similar to second order phase transitions (liquid to gas, ferro- or antiferro-magnet to paramagnet).

IV. CONCLUSION

Binding of a solvated peptide A1 with the graphene sheet is examined by a hierarchical coarse-grain simulation involving three independent simulated interaction potentials.[11,31,32] Results from three potentials show some common features as well as quantitative differences. Common findings include general binding patterns, i.e., the peptide is adsorbed at low temperatures and desorbed at high temperature. Adsorption to desorption transition can be described by the variation of the transverse component (R_{gy}) of the radius of gyration with the

temperature; R_{gy} could be a measure of the order parameter for the adsorption-desorption transition. The range of temperature over which the variation in the magnitude of the radius of gyration occurs can vary with the potentials.

Binding of the un-solvated peptide (A1) has been extensively studied by all-atom as well as coarse-grained simulations.[11,12] The un-solvated peptide can bind at low temperatures and unbind at high temperatures similar to solvated peptide. The binding strength of all residues in un-solvated peptide is about the same, although it is feasible to identify the residues that can bind with lower probability. The binding strength of residues in solvated peptide, on the other hand, is accentuated despite their reduced interaction[32] with the graphene. As a result it is easier to identify the residues ^{1}E, ^{4}Q, and ^{6}K that can anchor the binding of solvated peptide A1. There are quantitative differences in results from the three simulated potentials particularly the temperature range of the thermal response of the overall size (measured by the radius of gyration) of the peptide and therefore its structure and consequently their binding. Thermal response to binding strength (measured by N_g) of the anchoring residues (^{1}E, ^{4}Q, ^{6}K) also depends on the simulated potentials. While this study would be useful in interpreting the laboratory observations[2,11] it also suggests a need for multiple inputs particularly the force field, potential, and its implementation in assessing the reliability of qualitative and quantitative findings.

ACKNOWLEDGMENTS

This work is supported by the Air Force Research Laboratory (GR04691). N.D. and O.R. would like to acknowledge NSERC Discovery grant program (386018-2010). We thank Diana Lovejoy for reading the paper and corrections.

[1]Y. Cui, S. N. Kim, S. E. Jones, L. L. Wissler, R. R. Naik, and M. C. McAlpine, Nano Lett. **10**, 4559 (2010).
[2]S. N. Kim, Z. Kuang, J. M. Slocik, S. E. Jones, Y. Cui, B. L. Farmer, M. C. McAlpine, and R. R. Naik, J. Am. Chem. Soc. **133**, 14480 (2011).
[3]S. M. Tomasio and T. R. Walsh, J. Phys. Chem. C **113**, 8778 (2009).
[4]S. R. Whaley, D. S. English, E. L. Hu, P. F. Barbara, and A. M. Belcher, Nature (London) **405**, 665 (2000).
[5]M. Sarikaya, C. Tamerler, A. K. Y. Jen, K. Schulten, and F. Baneyx, Nat. Mater. **2**, 577 (2003).
[6]Y. Fang, Q. Wu, M. B. Dickerson, Y. Cai, S. Shian, J. D. Berrigan, N. Poulsen, N. Kroger, and K. H. Sandhage, Chem. Mater. **21**, 5704 (2009).
[7]M. J. Pender, L. A. Sowards, J. D. Hartgerink, M. O. Stone, and R. R. Naik, Nano Lett. **6**, 40 (2006).
[8]R. B. Pandey *et al.*, Phys. Chem. Chem. Phys. **11**, 1989 (2009).
[9]H. Heinz *et al.*, J. Am. Chem. Soc. **131**, 9704 (2009).
[10]L. F. Drummy *et al.*, ACS Appl. Mater. Interfaces **2**, 1492 (2010).
[11]R. B. Pandey, Z. Kuang, B. L. Farmer, S. S. Kim, and R. R. Naik, Soft Matter **8**, 9101 (2012).
[12]R. B. Pandey and B. L. Farmer, J. Chem. Phys. **139**, 164901 (2013).
[13]A. Chakrabarty and T. Cagin, Polymer **51**, 2786 (2010).
[14]A. E. van Giessen and J. E. Straub, J. Chem. Phys. **122**, 024904 (2005).
[15]D. Reith, M. Putz, and F. Muller-Plathe, J. Comput. Chem. **24**, 1624 (2003).
[16]R. B. Pandey, Z. Kuang, and B. L. Farmer, PLoS One **8**, e70847 (2013).
[17]A. Liwo, C. Czaplewski, J. Pillardy, and H. A. Scheraga, J. Chem. Phys. **115**, 2323 (2001).
[18]J. Zhou, I. F. Thorpe, S. Izvekov, G. A. Voth, Biophys. J. **92**, 4289 (2007).
[19]S. J. Marrink, H. J. Risselada, S. Yefimov, D. P. Tieleman, and A. H. de Vries, J. Phys. Chem. B **111**, 7812 (2007).
[20]Z. Wu, Q. Cui, and A. Yethiraj, J. Chem. Theory Comput. **7**, 3793 (2011).
[21]S. Tanaka and H. A. Scheraga, Macromolecules **9**, 945 (1976).
[22]S. Miyazawa, R. L. Jernigan, Macromolecules **18**, 534 (1985).
[23]M. R. Betancourt and D. Thirumalai, Protein Sci. **8**(2), 361 (1999).
[24]A. Godzik, A. Kolinski, and J. Skolnick, Proteins: Struct., Funct., Genet. **4**, 363 (1996).
[25]S.-Y. Huang and Z. Xiaoqin, Proteins: Struct., Funct., Genet. **79**, 2648 (2011).
[26]M. Fritsche, R. B. Pandey, B. L. Farmer, and D. Heermann, PLoS One **7**, e32075 (2012).
[27]R. B. Pandey and B. L. Farmer, PLoS One **7**, e49352 (2012).
[28]V. G. Sakai, S. Khodadadi, M. T. Cicerone, J. E. Curtis, A. P. Sokolov, and J. H. Roh, Soft Matter **9**, 5336 (2013).
[29]R. B. Pandey and B. L. Farmer, PLoS One **8**, e76069 (2013).
[30]M. Fritsche, R. B. Pandey, B. L. Farmer, and D. Heermann, PLoS One **8**, e64507 (2013).
[31]A. N. Camden, S. A. Barr, and R. J. Berry, "Simulations of peptide-graphene interactions in explicit water," J. Phys. Chem. B **117**, 10691 (2013).
[32]N. Dragneva, W. B. Floriano, D. Stauffer, R. C. Mawhinney, G. Fanchini, and O. Rubel, J. Chem. Phys. **139**, 174711 (2013).
[33]G. Nawrocki and M. Cieplak, Phys. Chem. Chem. Phys. **15**, 13628 (2013).
[34]J. Feng, R. B. Pandey, R. J. Berry, B. L. Farmer, R. R. Naik, and H. Heinz, Soft Matter **7**, 2113 (2011).
[35]I. Carmesin and K. Kremer, Macromolecules **21**, 2819 (1988).
[36]*Monte Carlo and Molecular Dynamics Simulations in Polymer Science*, edited by K. Binder (Oxford University Press, New York, 1995).